18TH WORLD CONFERENCE ON EARTHQUAKE ENGINEERING
WCEE2024
MILAN

MILAN, ITALY
30TH JUNE - 5TH JULY 2024
www.wcee2024.it

# PREDICTED AND RECORDED GROUND-BORNE VIBRATIONS INDUCED BY THE OPERATION OF TWO SHAKING TABLES AT THE NEW SOFSI RESEARCH FACILITY

Z. Zhang[1], R. De Risi[2], M. Dietz[3], D. Karamitros[4], D. Williams[5], T. Horseman[6], G. Mylonakis[7], A. Crewe[8] & A. Sextos[9]

[1] University of Southampton, Southampton, UK

[2] University of Bristol, Bristol, UK

[3] University of Bristol, Bristol, UK

[4] University of Bristol, Bristol, UK

[5] University of Bristol, Bristol, UK

[6] University of Bristol, Bristol, UK

[7] University of Bristol, Bristol, UK & Khalifa University, Abu Dhabi, United Arab Emirates

[8] University of Bristol, Bristol, UK

[9] University of Bristol, Bristol, UK & National Technical University of Athens, Athens, Greece, a.sextos@bristol.ac.uk

**Abstract**: *This work explores the ground vibrations induced by the 31 tonne, 6 m × 4 m, 3-degree-of-freedom (DOF) large shaking table and the 1 tonne, 1 m × 1 m, 6-DOF, high-acceleration "Hexapod" shaking table of the Soil-Foundation-Structure Interaction (SoFSI) Laboratory, Langford Campus University of Bristol, UK. A monitoring scheme was deployed during the operation and the triaxial acceleration responses are recorded at several locations within the university campus. The instrumentation is installed at both free-field conditions and at selected locations on the upper floors of nearby buildings. Acceleration time histories are also recorded on the shaking tables to back up table motions recorded internally by the control system. The latter are used as an input for a refined three-dimensional numerical model of a multi-layered soil volume of 400 m × 400 m × 30 m around the SoFSI building, including the exact geometry of the reinforced concrete reaction mass. The numerical model confirms the attenuation patterns of ground vibration within the area of Langford Campus as observed during field measurements. Epistemic uncertainties are further reduced by validating the measured and simulated data against analytical calculations; the kinematic response of a rigid SoFSI reaction mass is approximated utilising direct steady-state dynamics while vibration attenuation with distance is assessed using the Borntiz exponential decay model. The outcome of this monitoring campaign establishes confidence on the wave propagation attenuation with distance and frequency, and forms the basis for a digital twin for predicting vibrations on the buildings around the SoFSI Facility during operations at maximum performance. Using predictions of probable ground/structure vibration levels at sensitive locations within the campus, operational envelopes of the SoFSI shaking tables are determined so that disruptions in surrounding facilities are avoided.*

# 1 Introduction

The UK Collaboratorium for Research on Infrastructure and Cities (UKCRIC) Soil-Foundation-Structure Interaction (SoFSI) Laboratory (SoFSI, 2023) at the University of Bristol has two shaking tables (Figure 1). The first is a 1 m × 1 m, six degree-of-freedom (6-DOF), high-acceleration "Hexapod" shaking table (Sextos *et al.*, 2020) with 800 kg designed payload and designed peak acceleration capacity of 10.0 g at frequencies up to 120 Hz. The other is a 6 m × 4 m, 3-DOF shaking table with 50 tonne designed payload, capable of meeting the Telcordia (Bellcore) test standards (Telcordia, 2006) with acceleration capacity of 2.0 g at frequencies up to 50 Hz.

The SoFSI facility is located at the centre of the university's Langford Campus, surrounded by other various laboratories, teaching spaces, and offices (Figure 2). Following a preliminary study during the design phase (H. Su *et al.*, 2019), a monitoring scheme was employed to verify the level of perceivable vibrations within the campus when the shaking tables are in operation at maximum performance (in terms of acceleration, payload and pulse characteristics), during which the triaxial acceleration responses are recorded at various key locations. The instrumentation was installed at both free-field conditions and selected locations on the upper floors of nearby buildings, to correlate vibration intensity with human perception. Acceleration time histories were also recorded on the shaking tables themselves to back up table motions recorded internally by their control systems. The outcome of this monitoring campaign establishes confidence on the wave propagation attenuation characteristics with distance and frequency and forms a digital twin for predicting vibrations on the buildings around the SoFSI Facility when the shaking tables operate at maximum performance. By having information on the probable ground/structure vibration levels at sensitive locations within the campus, operational envelopes of the SoFSI shaking tables were determined so that disruptions to the surrounding facilities can be avoided.

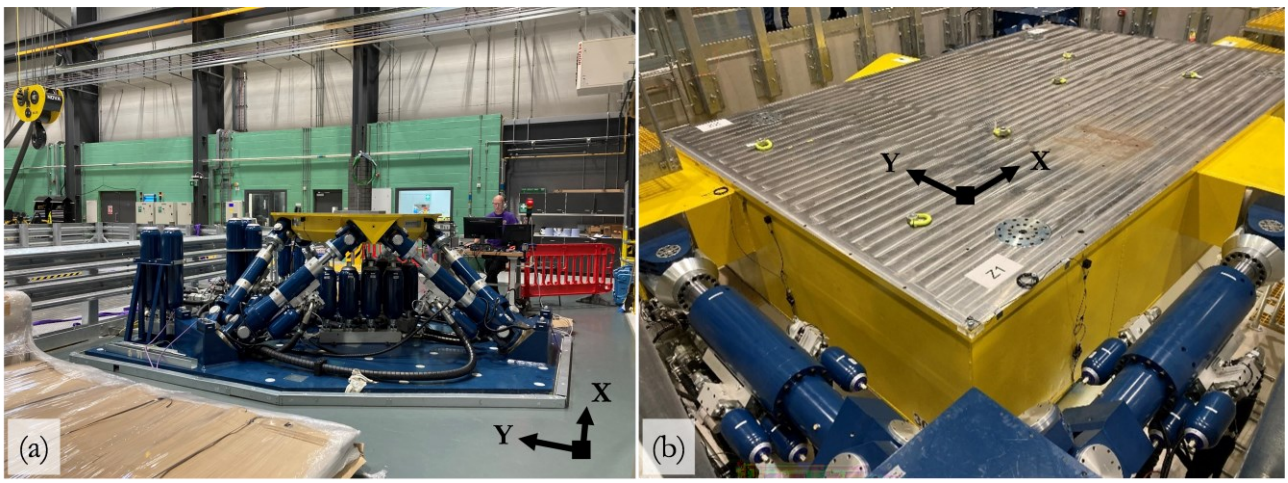


*Figure 1: Shaking tables in the SoFSI laboratory: (a) 1 m × 1 m Hexapod, (b) 6 m × 4 m shaking table.*

# 2 On-site vibration monitoring scheme

## 2.1 Monitoring scheme

Four types of instrumentation were deployed during on-site vibration monitoring, marked in different colours in Figure 2, namely: instrumentation on the shaking tables, on SoFSI strong floor, on open field, and on building upper floors. The shaking table motions were monitored by accelerometers (ASEDA MonStr (ASEDA, 2022)) mounted directly on the table platforms so to capture synchronised records of the actual accelerations produced. On the ground, accelerometers were installed both within the area of SoFSI reinforced concrete reaction mass and at selected locations away from the SoFSI reaction mass (i.e., free field) to monitor the attenuation of ground vibrations travelling within the reaction mass and beyond. These accelerometers are of the same model as those deployed on the shaking tables and use the same input/output channels (cable connected), thus enabling high-quality, synchronised acceleration time history recordings. On the other hand, mobile phones with built-in accelerometers were utilised to take acceleration measurements on the upper floors of selected nearby buildings, marked with green crosses in Figure 2. Below 1 gal (1 gal = approx. 0.01

m/s$^2$) of ambient noise was measured by all ASEDA sensors (mobile phones records slightly higher noises not exceeding 1.5 gal), confirming the consistency of signal-to-noise-ratio of all measurements.

Apart from quantitative measurements, qualitative evaluations of human perception to vibration were made possible via coordinated staff feedbacks. A survey form was made available to university staff within the campus to report any perceived vibrations during the days of on-site monitoring at maximum performance, when the shaking tables were put into action in time periods unknown to university staff outside of SoFSI facility. The collected information includes the perceived time and location of vibration, as well as descriptions of human perception or object rattling or moving. For determining the correlation between human perception to vibration with respect to the acceleration amplitude, staff comments are associated with site measurements or calibrated numerical predictions.

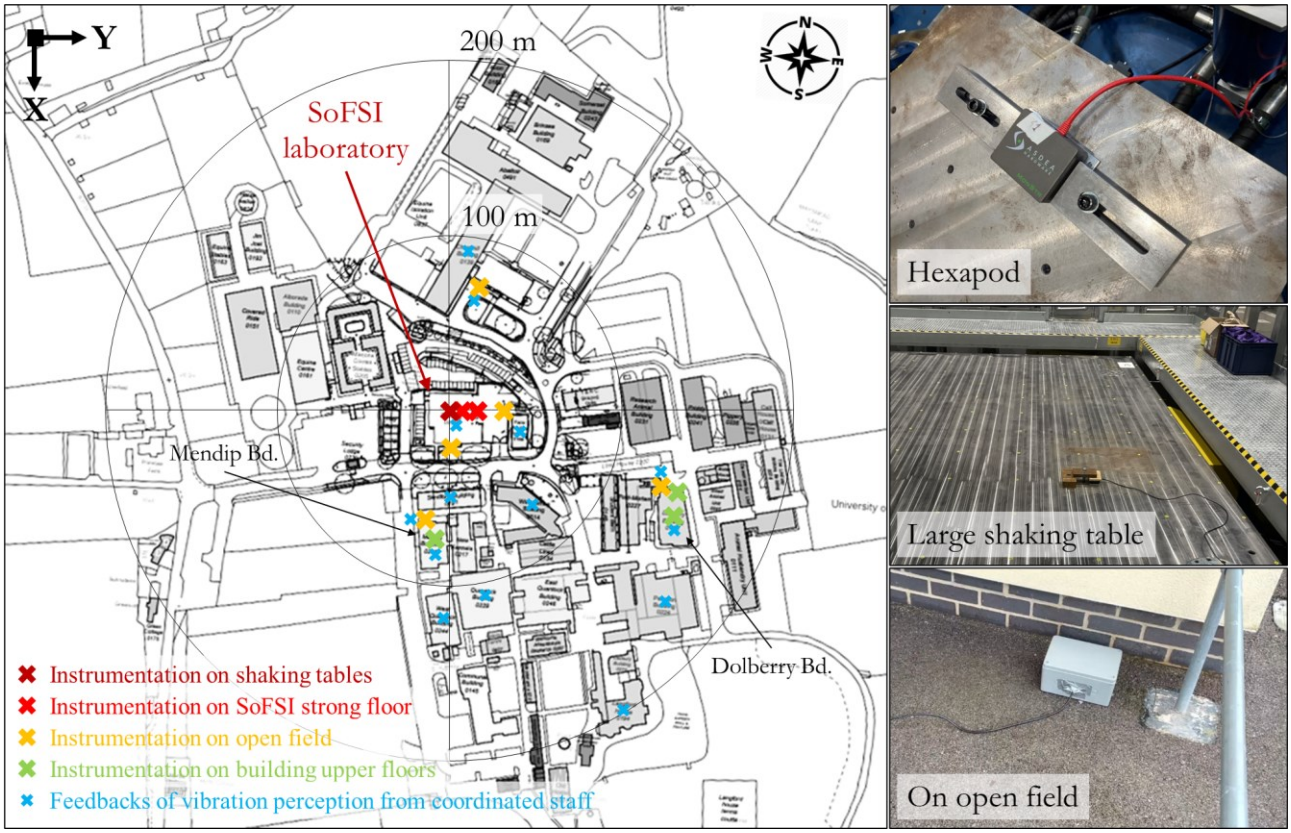


*Figure 2: Site layout and instrumentation.*

### 2.2 Shaking table excitations

The on-site vibration monitoring campaigns for the two shaking tables were conducted independently, and the shaking tables are tested a variety of time history inputs. In this paper, two extreme-case scenario excitations produced by each of the shaking tables are demonstrated as examples. For the Hexapod, the worst-case scenario input is a 6-axis spectrum-compatible excitation with peak acceleration up to 15 g with targeted excitation frequency band of 8 to 11 Hz (Figure 3, a), which is produced during an extreme headroom verification test of the Hexapod and the induced vibration is perceived by university staff on the first floor of a nearby Building, located some 70 m away from the SoFSI facility (Figure 2). For the large shaking table, the most critical input excitation is a 2.0 g amplitude, x-axis, sine sweep excitation with frequency bands ranging from 0.78 to 50 Hz separated by half-octaves (Figure 3, b), which also mobilises the full power of the shaking table and is perceived by university staff on the second floor of a second Building (Figure 2). Both these excitations are very rarely generated on the shaking tables in real life operation of the SoFSI facility.

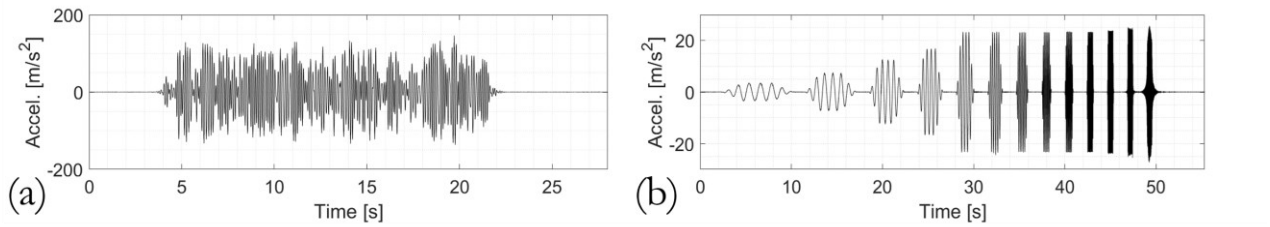


*Figure 3: Worst-case scenario shaking table excitations for the two shaking tables: (a) 15 g peak acceleration, 6-axis spectrum-compatible excitation produced by the Hexapod shaking table and (b) 2.0 g peak acceleration, x-axis, sine sweep excitation produced by the 6 m × 4 m large shaking table.*

### 2.3 Ground acceleration attenuation

The attenuation of acceleration amplitude in the free field as a function of distance to the centre of SoFSI reaction mass is summarised in Figure 4. Least-squares regressions were performed to fit first order exponential functions for each response component and the overall magnitude of three-axis ground acceleration response. A horizontal dashed line at acceleration of 10 gal (i.e., 0.1 m/s$^2$) is marked as an indication of an approximate threshold for vibration perception, which is based on authors' experience during the monitoring campaign. More information on vibration perception is provided in (Richart, 1970)

For the Hexapod shaking table with 15 g amplitude spectrum-compatible excitation, it was found that ground response near the Hexapod is approximately 60 gal, which decays to 50 % at a distance of 25 m, and 25 % at 55 m. While the ground acceleration level at the location of the Mendip Building (around 70 m away from the centre of the SoFSI facility) is supposed to be just barely perceivable, the dynamics of the building and the floor are likely to contribute to significant amplification. As a rule of thumb, building dynamics may approximately amplify the ground motion by a factor of 2.5. This estimate is based on Eurocode 8 elastic response spectrum (CEN, 2004), in which the constant spectral acceleration branch (applicable for common low-rise buildings) is 2.5 times the peak ground acceleration. The potential of acceleration amplification during this particular test is further highlighted by the frequency content of this Hexapod excitation (8 to 12 Hz) which coincides with the estimated second natural frequency of the soil deposit (approximately 12 Hz), as well as the vibration frequency band to which humans are particularly sensitive [4 to 12 Hz (Corlett, 1989; Malerbi, 1989; BSI, 2008)]. Another interesting observation from this figure is that the attenuation of acceleration response is evident even within the strong floor.

For the 2g amplitude sine sweep excitation produced by the large shaking table, the magnitude of ground acceleration in the close proximity of the shaking table is measured at approximately 100 gal. The maxima of x-axis accelerations are reduced by 50% at a distance of around 25 m and decayed to a quarter at a distance of around 50 m. It is noted that while the amplitudes of x- and y-axis ground acceleration response are comparable near the shaking table pit, attenuation of y-axis response with distance is much quicker. The z-axis response has minor contribution to the overall response magnitude given that the large shaking table does not produce vertical acceleration. It is vertically supported only on four high-pressure hydraulic oil slipper pads to accommodate lateral movements.

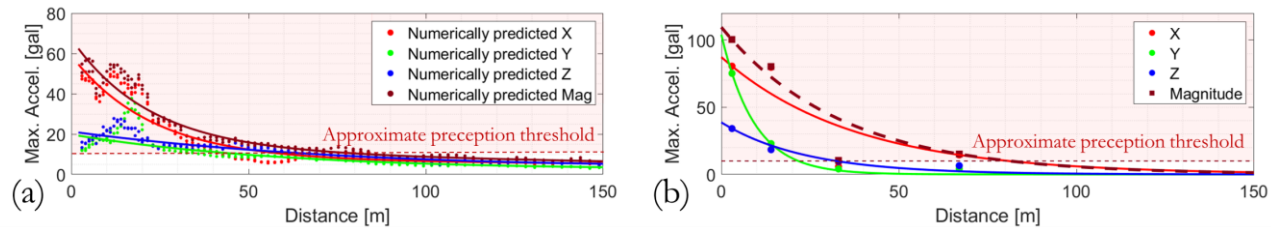


*Figure 4: Acceleration amplitude attenuation from the centre of the SoFSI reaction mass produced by case study excitations from (a) the Hexapod shaking table (results from calibrated digital twin is substituted given the lack of experimental data on this extreme case) and (b) measured accelerations during the 6 m × 4 m large shaking table 2.0g test.*

# 3 Analytical prediction of shaking table-induced vibration and attenuation

Two-dimensional analytical solution (in the y-z plane of Figure 2) of the maximum and the attenuation of ground acceleration induced by harmonic excitations on the surface of an assumed rigid rectangular foundation, fully embedded in a two-layer soil deposit, is given in this section. By making a comparison to the experimentally measured results, the analytical solution aims at reducing epistemic uncertainties to the problem and gain further confidence in bridging the results of the on-site monitoring scheme to those of the digital twin.

## 3.1 Response of a two-dimensional rectangular foundation subjected to sinusoidal excitation

The two shaking tables, assumed to be nodal masses at the surface of the foundation being excited horizontally by harmonic excitations, are examined independently: (a) the Hexapod shaking table has equivalent moving mass $m_m$ = 2 Mg and peak acceleration $a_m$ = 15g, and (b) the large shaking table has equivalent moving mass $m_m$ = 31 Mg and peak acceleration $a_m$ = 2g. The excitation frequency is set at $f$ = 10 Hz, which is the (or part of the) targeted excitation frequencies of both cases and is a vibration frequency to which human are particularly sensitive (Corlett, 1989; Malerbi, 1989; BSI, 2008). The reaction mass is assumed to be rigid with x-, y-, and z-axis dimensions of $2X \times 2Y \times Z$ = 12 m × 23 m × 5 m and equivalent mass $m$ = 2500 Mg . The reaction mass is fully embedded in a 5 m deep layer of soil with shear wave velocity $V_s$ = 150 m/s, underlain by a half-space with $V_s$ = 300 m/s. Both soil layers have Poisson's ratio $v$ = 0.3, unit weight $\gamma_{soil}$ = 18kN/m$^3$, and material damping $\xi$ = 2 %.

The two-dimensional analytical solution of reaction mass acceleration response $a_{y0}$ subjected to horizontal and harmonic shaking table excitation at its surface is calculated as follows:

$$a_{y0} = \omega^2 \cdot u_{y0} \tag{1}$$

$$u_{y0} = u_{y0,base} + \theta_{x0,base} \cdot Z \tag{2}$$

$$\begin{bmatrix} u_{y0,base} \\ \theta_{x0,base} \end{bmatrix} = \left\{ \begin{bmatrix} K_y & K_{y,rx} \\ K_{y,rx} & K_{rx} \end{bmatrix} + i\omega \begin{bmatrix} C_x & C_{y,rx} \\ C_{y,rx} & C_{rx} \end{bmatrix} - \omega^2 \begin{bmatrix} m & m\frac{Z}{2} \\ m\frac{Z}{2} & I_x \end{bmatrix} \right\}^{-1} \begin{bmatrix} m_m a_m \\ m_m a_m Z \end{bmatrix} \tag{3}$$

where $a_{y0}$ is the amplitude of total horizontal acceleration at the surface of reaction mass; $\omega = 2\pi f$ is the circular frequency; $u_{y0}$ is the amplitude of total displacement at the surface of reaction mass; $u_{y0,base}$ is the base horizontal displacement; $\theta_{x0,base}$ is the base rotation; $K_y$, $K_{rx}$, and $K_{y,rx}$ are the horizontal, rocking, and swaying-rocking coupled dynamic stiffnesses, which are frequency dependent; $C_y$, $C_{rx}$, and $C_{y,rx}$ are the corresponding dashpot coefficients; and $I_x$ is the mass moment of inertia of the foundation about the x-axis, i.e., the axis perpendicular to the two-dimensional reaction mass. To facilitate the calculation of equivalent stiffness and dashpot coefficients of layered soil, each of the six dynamic stiffness and dashpot coefficients are further estimated following a superposition scheme introduced by Su et al (2019), as illustrated in Figure 5. An example is given for horizontal dynamic stiffness coefficient $K_y$:

$$K_y = K_y^{surf,2} + K_y^{emb,1} - K_y^{surf,1} \tag{4}$$

the superscripts *surf* or *emb* represent relevant quantities for foundations atop or be embedded in the labelled soil layer, *1* or *2*. The dynamic stiffness and dashpot coefficients are calculated following (Gazetas, 1991; Mylonakis, Nikolaou and Gazetas, 2006).

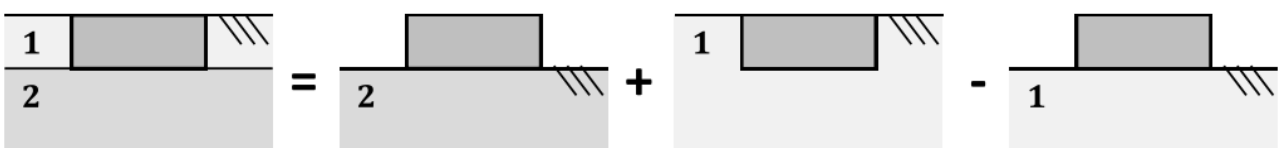


*Figure 5: Illustration of the superposition rule for calculating equivalent stiffness and dashpot coefficients given layered soil (after Su et al 2019).*

### 3.2 Analytical solution of vibration amplitude attenuation

The attenuation of peak acceleration response $a_{y0}$ at the surface of the reaction mass can then be approximated analytically using a power law-exponential decaying model originally proposed by Bornitz (Bornitz, 1931):

$$\left|\frac{a_i}{a_{y0}}\right| = \left(\frac{R}{r}\right)^{\gamma_1} e^{-\alpha\left(\frac{r-R}{R}\right)} \tag{5}$$

$$\alpha = \gamma_2 \xi \left(\frac{\omega R}{V_R}\right) \tag{6}$$

where $a_i$ is the surface acceleration amplitude of ground vibration along the distance $r$; $R$ is the characteristic half length of the foundation, which can be represented by $R = Y = 11.5$ m in this study; $\gamma_1 = 0.5$ is a calibrated geometric damping factor (Huize Su *et al.*, 2019); $\alpha$ is a material damping factor; $\gamma_2 = 0.8$ is a calibrated loss factor for characterising the attenuation pattern (Su *et al.*, 2019); $V_R$ is the Rayleigh wave velocity of the homogeneous soil which can be approximated by $V_R \approx 0.927 \cdot V_s$ for linear elastic material with Poisson's ratio $v = 0.3$ (Towhata, 2008), assuming $V_s = 150$ m/s for the purpose of estimating the factor $\alpha$. The $V_s$ corresponding to the upper soil layer is used in this calculation because Rayleigh wave, which travels close to the ground surface, is believed to be most relevant to the problem.

### 3.3 Analytically predicted acceleration attenuation

The above calculations are performed for both the Hexapod and the large shaking table, of which the results are shown in Figure 6. The analytical solutions indicate that the approximate range of perceptible vibrations in the open field is at the order of 50 m and 75 m for the Hexapod and the large shaking table respectively. The calculated acceleration amplitude attenuation profile beyond the assumed-rigid SoFSI reaction mass is considered in good agreement with site measurements (Figure 4, b) given the various simplifications made during the analytical calculation - especially by ignoring the elasticity and the cavities in the SoFSI reaction mass, as well as the complexity of the real soil strata.

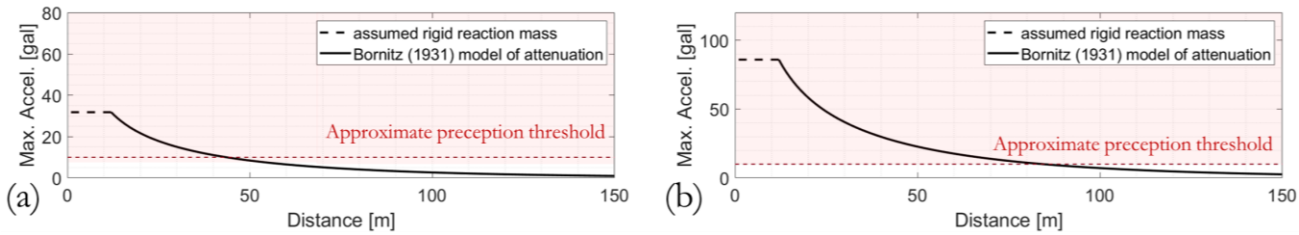


*Figure 6: Analytically calculated acceleration attenuation from the centre of the SoFSI reaction mass produced by case study excitations from (a) the Hexapod shaking table and (b) the 6 m × 4 m large shaking table according to the attenuation model in equations 5 and 6.*

## 4 A digital twin for predicting shaking-table induced vibrations

### 4.1 Site response

The Langford Campus within a 400 m × 400 m area is modelled in a site response analysis model (Figure 7) using OpenSees (*OpenSees Documentation*, 2022) in combination with STKO (ASDEA software, 2021). The assumed soil stratigraphy comprises vertically layered soil starting with shear wave velocity ($V_s$) of 200 m/s at the surface and increasing by 100 m/s for every 5 meters of depth. The reaction mass is idealised as a 12 m × 23 m × 5 m cuboid of reinforced concrete with two cavities representing the 8 m × 6 m × 4 m large shaking table pit and a 6 m × 5 m × 4 m soil pit. Additionally, a 30 m × 50 m × 5 m zone of disturbed soil ($V_s = 150$ m/s) located concentrically around the reaction mass is considered, taking into account the volume of soil excavated and backfilled during construction of the facility. Rayleigh damping is employed with the mass and stiffness proportional coefficients determined by matching the derived Rayleigh damping curve to the typical small-strain damping ratio of soil, which is around 1.0 % (Vucetic and Dobry, 1991; Senetakis and Madhusudhan, 2015; Khan *et al.*, 2018; Mog and Anbazhagan, 2022), near the frequency range 4 to 12 Hz, where whole body vibration of human is most probable due to potential high spinal loads (Corlett, 1989; Malerbi, 1989) and

resonance within body cavity (Grether, 1971). The soil domain is surrounded by absorbing boundaries, which incorporate the free-field column concept (Zienkiewicz, Bicanic and Shen, 1989), the Lysmer-Kuhlemeyer viscous boundary (Lysmer and Kuhlemeyer, 1969), as well as the boundary tractions transferred from the free-field to the modelled soil domain. Shaking table excitations are converted to equivalent force time histories imposed at four corners of the Hexapod base or the mounting points of the dynamic actuators for the large shaking table. The analysis is linear visco-elastic given the expectedly low amplitude of accelerations associated with machine-induced vibrations.

The numerically predicted acceleration amplitude attenuation profiles are compared against their experimentally measured counterparts for a variety of shaking table inputs. An example is shown in Figure 8 for the 2g amplitude, sine sweep excitation conducted on the large shaking table. The digital twin confirmed an acceleration amplitude of about 100 gal near the shaking table pit, and a ground acceleration amplitude dominated by the response along the x-axis. The simulated acceleration attenuation over horizontal distance agrees well with both the experimental measurements and the analytical solution. It is noted that the numerically predicted acceleration amplitudes vary significantly between various locations within the reaction mass due to both the elasticity of the reaction mass (material) and the existence of the two pits (geometry). This is confirmed by repeating the numerical analysis on a reaction mass modelled as rigid and/or without the cavities.

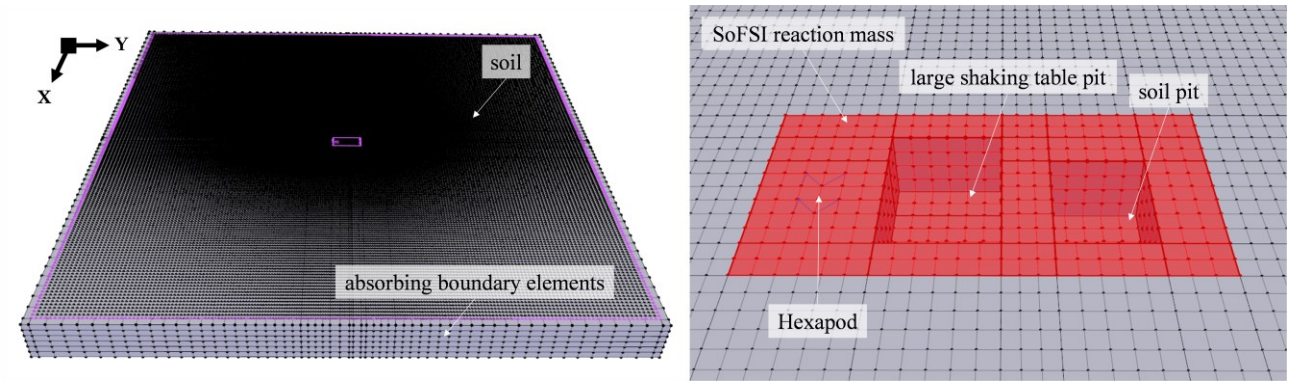


*Figure 7: Site response model reflecting the SoFSI reaction mass and the nearby areas in Langford Campus, University of Bristol.*

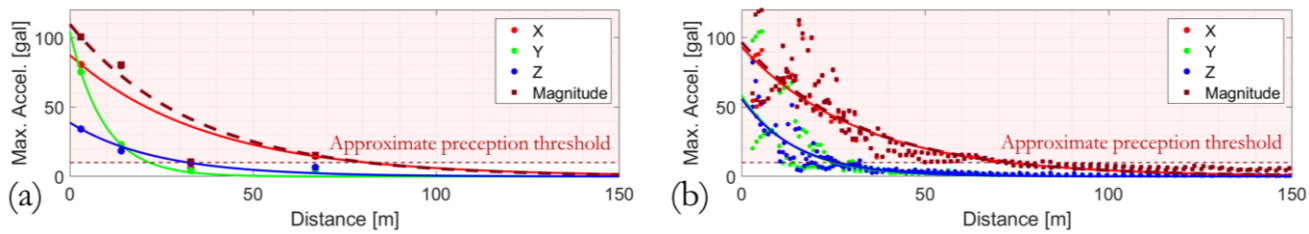


*Figure 8: Comparison of acceleration amplitude attenuation results of the 2g sine sweep excitation on the large shaking table: (a) measured by means of deployed instrumentation, (b) numerically predicted.*

### 4.2 Structural response

To predict the on-floor vibration responses at nearby buildings, it is essential to accurately model the overall dynamics of buildings by capturing explicitly the out-of-plane stiffnesses of the floor diaphragms using shell finite elements. This is because an amplification of ground accelerations is probable on the upper floors as the result of both overall structural resonance and local floor flexibility, especially in the vertical direction (Chopra, 2012). Input to a floor response analysis is the three-axis ground acceleration time history at the location of the building, obtained from site response analysis. Soil structure interaction and wave travel effect are ignored in these analyses. Appropriate Rayleigh damping, such as 5 % for reinforced concrete structures, is applied based on the fundamental and second natural frequencies of the buildings. As an example, the shell element model of Dolberry Building and its second-floor maximum acceleration response contour during the case study

test on the large shaking table is given in Figure 9. The predicted on-floor time history responses can then be used to assess vibration perceptions.

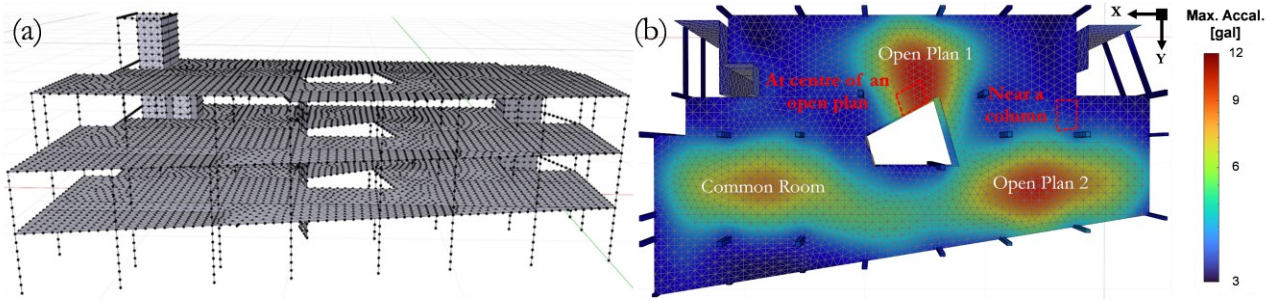


*Figure 9: (a) Structural model of Dolberry Building, (b) maximum acceleration on the second floor during the 2 g sine sweep excitation on the large shaking table.*

## 5 Conclusions

This study investigated experimentally, analytically, and numerically the vibrations induced by two shaking tables installed in the University of Bristol Soil-Foundation-Structure Interaction (SoFSI) Laboratory. An on-site monitoring scheme was carried out to measure the vibration levels at various key locations around the university campus. Confidence on the experimental measurements was enhanced by its fair agreement to an analytical solution of the peak and the attenuation of ground acceleration induced by harmonic excitations on the surface of an assumed rigid rectangular foundation. A digital twin of the SoFSI facility and the Langford Campus was then developed for predicting on-site/on-floor acceleration responses. The two-stage analysis procedure comprises a solid element site response analysis model, reflecting the reinforced concrete reaction mass of the SoFSI facility and the adjacent soil domain covering the entire area of the Langford Campus, followed by a shell element structural analysis model for the building of interest. The numerical results confirm the trends of acceleration amplitude attenuation over the distance observed from measurements and the predicted on-floor peak accelerations matched well with what measured experimentally during the tests. The validated digital twin is then utilised to predict ground/on-floor acceleration responses at various other locations not monitored during the experimental campaign for various other shaking table testing scenarios, such as for other shaking table excitations or with different payload levels.

The overall results indicate that ordinary use of both the shaking tables are unlikely to cause disturbance anywhere within the Langford Campus. This, as a general conclusion, is backed up by the fact that the SoFSI facility had since operated normally for more than a year. Exceptionally, it could be possible that vibrations may be perceived at particular locations, most probably on the upper floors of nearby buildings, when extreme testing scenarios such as high acceleration motions with specific frequency contents (around 10 Hz) are replicated on the large shaking table with heavy payloads, or on the Hexapod shaking table with boosted performance for ultra-high accelerations.

## 6 References

ASDEA software (2021) ‘Scientific Toolkit for OpenSees (STKO) User Manual’, pp. 1–228.

ASEDA (2022) *MonStr (Monitoring Structural) system*. Available at: https://asdea.eu/hardware/monstr-system/ (Accessed: 23 October 2022).

Bornitz, G. (1931) *Über die Ausbreitung der von Großkolbenmaschinen erzeugten Bodenschwingungen in die Tiefe (in German)*. Springer Berlin, Heidelberg. Available at: https://doi.org/0.1007/978-3-642-99597-2.

BSI (British Standards Institution) (2008) *Guide to evaluation of human exposure to vibration in buildings (1 to 80 Hz) - Part 1: Vibration sources other than blasting*. UK. Available at: https://knowledge.bsigroup.com/products/guide-to-evaluation-of-human-exposure-to-vibration-in-buildings-vibration-sources-other-than-blasting/standard.

CEN (European Committee for Standardisation) (2004) *Eurocode 8: Design of structures for earthquake resistance - Part 1: General rules, seismic actions and rules for buildings*. Brussels: EN 1998-1:2004 (E).

Chopra, A.K. (2012) *Dynamic of Structures: Theory and Applications to Earthquake Engineering*. Fourth Edi, *Prentice-Hall International Series in Civil Engineering and Engineering Mechanics*. Fourth Edi. Edited by W.J. Hall. Prentice Hall.

Corlett, E.N. (1989) 'Chapter 20 - Ergonomics', in H.A. Waldron (ed.) *Occupational Health Practice*. Third Edit. Elsevier Ltd., pp. 375–391. Available at: https://doi.org/10.1016/B978-0-407-33702-2.50025-7.

Gazetas, G. (1991) 'Formulas and Charts for Impedances of Surface and Embedded Foundations', *Journal of Geotechnical and Geoenvironmental Engineering, ASCE*, 117(9), pp. 1363–1381. Available at: https://doi.org/10.1061/(ASCE)0733-9410(1991)117:9(1363).

Grether, W.F. (1971) 'Vibration and Human Performance', *Human Factors: The Journal of the Human Factors and Ergonomics Society*, 13(3), pp. 203–216. Available at: https://doi.org/10.1177/001872087101300301.

Khan, M.A. *et al.* (2018) 'Analysis of restrained composite beams exposed to fire using a hybrid simulation approach', *Engineering Structures*, 172(June), pp. 956–966. Available at: https://doi.org/10.1016/j.engstruct.2018.06.048.

Lysmer, J. and Kuhlemeyer, R.L. (1969) 'Finite Dynamic Model for Infinite Media', *Journal of the Engineering Mechanics Division*, 95(4), pp. 859–877. Available at: https://doi.org/10.1061/JMCEA3.0001144.

Malerbi, B. (1989) 'Chapter 6 - Vibration', in H.A. Waldron (ed.) *Occupational Health Practice*. Third Edit. Elsevier Ltd., pp. 101–112. Available at: https://doi.org/10.1016/B978-0-407-33702-2.50011-7.

Mog, K. and Anbazhagan, P. (2022) 'Evaluation of the damping ratio of soils in a resonant column using different methods', *Soils and Foundations*, 62(1), p. 101091. Available at: https://doi.org/10.1016/j.sandf.2021.101091.

Mylonakis, G., Nikolaou, S. and Gazetas, G. (2006) 'Footings under seismic loading: analysis and design issues with emphasis on bridge foundations', *Soil Dynamics and Earthquake Engineering*, 26(9), pp. 824–853.

*OpenSees Documentation* (2022). Available at: https://opensees.github.io/OpenSeesDocumentation/index.html (Accessed: 24 September 2022).

Richart, F.E. (1970) *Vibrations of Soils and Foundations*. Englewood Cliffs, N.J: Prentice-Hall.

Senetakis, K. and Madhusudhan, B.N. (2015) 'Dynamics of potential fill–backfill material at very small strains', *Soils and Foundations*, 55(5), pp. 1196–1210. Available at: https://doi.org/10.1016/j.sandf.2015.09.019.

Sextos, A.G. *et al.* (2020) 'Design of a high-performance Hexapod shaking table to meet the requirements in the latest seismic qualification codes', in *17th World Conference of Earthquake Engineering*. Sendai, Japan, pp. 1–12.

SoFSI (2023) *The UKCRIC Soil-Foundation-Structure Interaction Laboratory*. Available at: https://sofsi.bristol.ac.uk/ (Accessed: 24 September 2022).

Su, H. *et al.* (2019) 'TRANSMISSION OF FOUNDATION VIBRATIONS', in *2019 SECED Conference, 9-10 September 2019, Greenwich, London*. Available at: http://www.bristol.ac.uk/red/research-policy/pure/user-guides/ebr-terms/.

Su, Huize *et al.* (2019) 'Transmission Of Foundation Vibrations', in *Earthquake risk and engineering towards a resilient world*. Greenwich, London, UK, pp. 1–11. Available at: https://research-information.bris.ac.uk/en/publications/transmission-of-foundation-vibrations.

Telcordia (2006) *NEBS Requirements: Physical Protection*. USA: GR-63-CORE.

Towhata, I. (2008) *Geotechnical Earthquake Engineering*. Edited by W. Wu and R.I. Borja. Springer, Berlin, Heidelberg. Available at: https://doi.org/10.1007/978-3-540-35783-4.

Vucetic, M. and Dobry, R. (1991) 'Effect of Soil Plasticity on Cyclic Response', *Journal of Geotechnical Engineering*, 117(1), pp. 89–107. Available at: https://doi.org/10.1061/(ASCE)0733-9410(1991)117:1(89).

Zienkiewicz, O.C., Bicanic, N. and Shen, F.Q. (1989) 'Earthquake Input Definition and the Trasmitting Boundary Conditions', in *Advances in Computational Nonlinear Mechanics*. Vienna: Springer Vienna, pp. 109–138. Available at: https://doi.org/10.1007/978-3-7091-2828-2_3.